ChemPubSoc Europe

DOI: 10.1002/chem.201603617

CHEMISTRY
A European Journal
Full Paper

Fluorescence Probes

Fluorogenic Behaviour of the Hetero-Diels–Alder Ligation of 5-Alkoxyoxazoles with Maleimides and their Applications

Kévin Renault,[a] Laurie-Anne Jouanno,[b] Antoine Lizzul-Jurse,[a] Pierre-Yves Renard,[a] and Cyrille Sabot*[a]

Abstract: Fluorogenic reactions are largely underrepresented in the toolbox of chemoselective ligations despite their tremendous potential, particularly in chemical biology and biochemistry. In this respect, we have investigated in full detail the fluorescence behaviour of the azaphthalamide, a scaffold which is generated through a hetero-Diels–Alder reaction of 5-alkoxyoxazole and maleimide derivatives under mild conditions that are compatible with, among others, peptide chemistry. The scope and limitations of such a fluorogenic labelling strategy were examined through four distinct applications, which target enzymatic activities or bioorthogonal reactions.

Introduction

Chemoselective ligation chemistry has dramatically gained importance in recent years, which provides fascinating opportunities in different research fields, including material and life sciences.[1] It involves reliable covalent bond formation, which takes place specifically between two chemical handles under mild conditions and avoids significant interference with biological functional groups. This strategy enables effective construction of (bio)molecular structures that span from simple scaffolds to complex molecular architectures, which is enabled by, among other characteristics, their broad functional group tolerance and reaction condition tolerability.[2]

Different ligation strategies have been proposed over the years, and condensation reactions of hydrazines/alkoxyamines with carbonyl derivatives to provide the corresponding hydrazones/oximes were among the first chemoselective ligations to be reported.[3] Azides have proven to be a particularly effective reaction partner, first with triarylphosphines in the Staudinger ligation,[4] and then with alkynes in the copper-catalyzed azide–alkyne cycloaddition (CuAAC).[5] Later on, strain-promoted azide–alkyne (SPAA),[6] alkyne–sydnone,[7] and alkyne–cyclic nitrone cycloaddition (SPANC)[8] were developed to circumvent the use of toxic copper catalysts. Several other ligation strategies have been proposed, which include inverse-electron-demand Diels–Alder reactions between tetrazines and strained alkenes[9] and between *o*-quinone methides and vinyl thioethers.[10]

Specifically, some ligation strategies have been used to design molecular biosensors and bioprobes for real-time monitoring of biological events or enzymatic assays suitable for high-throughput screening or biomedical imaging applications.[11] The preparation of such biomolecular systems mostly relies on a fluorescent labelling step, which involves chemoselective ligation tools. In most cases, a fluorescent dye is required on the ligation partner to label the molecule of interest; however, there are a few scarce examples of fluorogenic reactions[12] that enable the formation of fluorescent linkages, such as the aldehyde–amino benzamidoxime ligation,[13] the tetrazole–alkene photoclick chemistry,[14] or azide–cyclooctyne ligation with specifically designed cyclooctynes.[15]

We recently reported the Kondrat'eva ligation, an irreversible-based Diels–Alder reaction between 5-alkoxyoxazole and maleimide derivatives, which led to the formation of an azaphthalimide linker.[16,17] Interestingly, this irreversible two-step reaction, which involves a Diels–Alder reaction followed by an aromatization step with concomitant release of ethanol, occurred in a single-step protocol either in the presence of a few

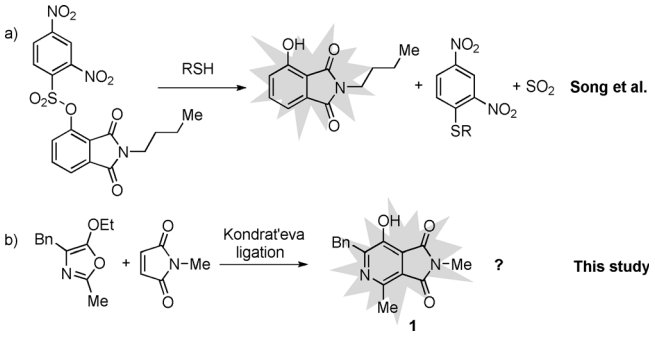

Scheme 1. Phthalimide and azaphthalimide derivatives.

[a] K. Renault, A. Lizzul-Jurse, Prof. Dr. P.-Y. Renard, Dr. C. Sabot
Normandie University, CNRS, UNIROUEN, INSA Rouen
COBRA (UMR 6014), 76000 Rouen (France)
E-mail: cyrille.sabot@univ-rouen.fr

[b] Dr. L.-A. Jouanno
Department of Chemistry and Biomolecular Sciences
University of Ottawa, 10 Marie Curie, Ottawa, Ontario, K1N 6N5 (Canada)

Supporting information and the ORCID identification number(s) for the author(s) of this article can be found under:
http://dx.doi.org/10.1002/chem.201603617.

equivalents of trifluoroacetic acid (TFA) in the medium or in a sodium acetate buffer (pH 5.0). Shortly after publishing our article, Song et al. reported a phthalimide-based fluorescent probe for the detection of biothiols (Scheme 1 a).[18] Their result led us to examine whether the azaphthalimide scaffold that is generated during the ligation process would be fluorescent, and if so, to what extent (Scheme 1 b). Herein, we report the detailed investigation of the photophysical properties of azaphthalimide scaffolds along with their direct applications in the synthesis of biologically relevant fluorogenic probes.

Results and Discussion

Study of photophysical properties of azaphthalimides

The optical behaviour of the azaphthalimide scaffold (i.e., solvent and pH effect) was determined by using the model compound **1**. First, absorption and emission spectra were recorded in various solvents, which ranged from nonpolar aprotic to polar protic medium (Figure 1 a).

In weakly ionizing solvents, such as toluene or dichloromethane, an absorption band at ≈350 nm was mainly observed. In contrast, in polar aprotic and polar protic solvents, such as DMF, MeOH, or water, a new absorption peak was detected above 400 nm along with a decrease in the intensity of the band at ≈350 nm. From these positive solvatochromic results, it was assumed that the high- and low-energy absorption band could be assigned to neutral and ionized azaphthalimide species, respectively. In fact, polar media would favor the formation of a hydrogen-bonding interaction between the hydroxyl group of the azaphthalimide moiety and the solvent. To further investigate this hypothesis, the influence of the deprotonation of the hydroxyl group of azaphthalimide **1** on the absorption and fluorescence emission spectra was investigated in the nonpolar toluene solvent (Figure 1 b–d). The absorption peak at ≈350 nm decreased gradually upon the addition of 1,8-diazabicyclo[5.4.0]undec-7-ene (DBU), and the appearance of a red-shifted absorption band was observed at ≈420 nm. Moreover, the gradual disappearance of the fluorescence emission that corresponded to an excitation in the high-energy absorption band (350 nm) was observed, and a band at ≈520 nm appeared. Besides, a noticeable increase in the emission peak intensity at ≈520 nm under an excitation wavelength of 430 nm was observed. Collectively, these data suggest that the neutral azaphthalamide species absorbs at 350 nm and emits at 420 nm, and the phenolate species absorbs at 420 nm and emits at 520 nm. These results are also confirmed by the analysis of their excitation spectra recorded at 420 and 520 nm (see the Supporting Information). In most of the aforementioned solvents (except toluene and dichloromethane), both phenol and phenolate species are present in the reaction medium, albeit in different proportions. Furthermore, the phenolic form of the azaphthalimide generally exhibits a significantly weaker fluorescence at 420 nm than its phenolate counterpart at 520 nm. Indeed, deprotonation of the hydroxyl group increases the electron density within the aromatic ring system and then enhances the intramolecular charge transfer (ITC) process, which is likely responsible for fluorescence emission. Consequently, the absorption and emission behaviour of the azaphthalimide scaffold was investigated in aqueous media at different pH values to determine the suitability of the azaphthalimide scaffold for future fluorescence applications.

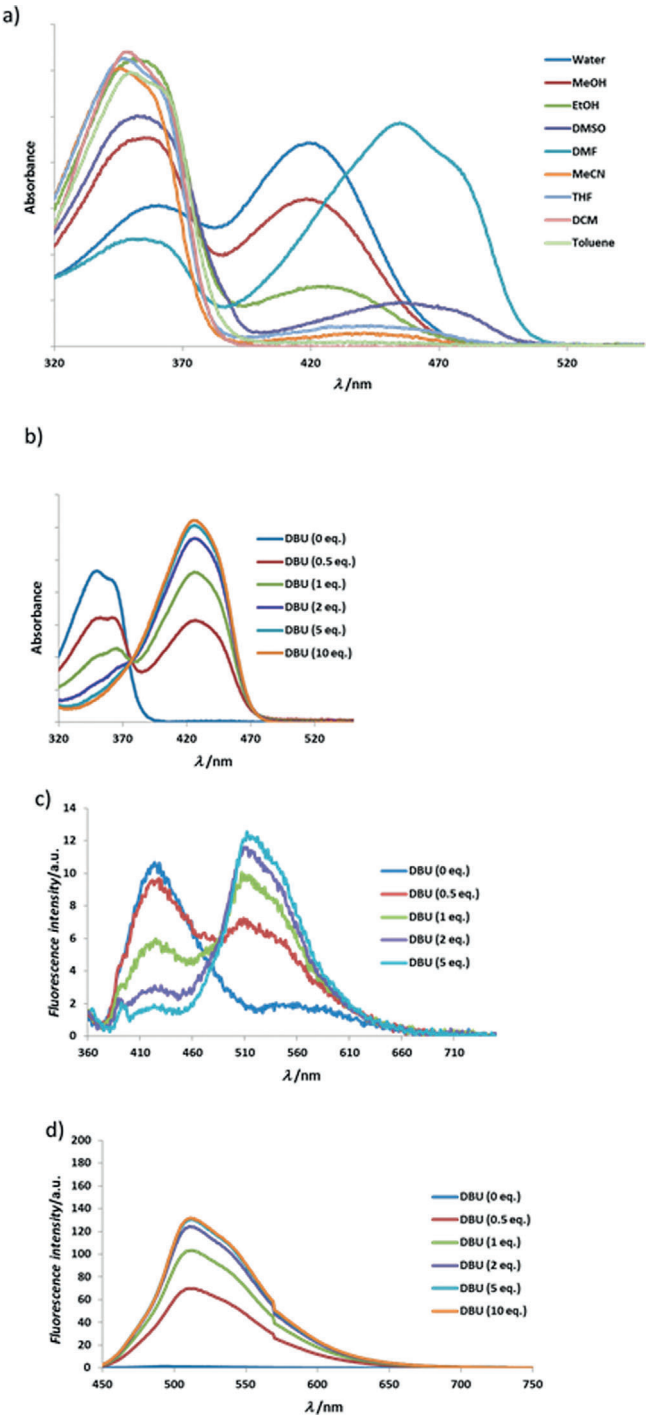

Figure 1. Photophysical behaviour of compound **1**. a) Absorption spectra in different solvents and b) in toluene in the presence of different amounts of DBU at 25 °C. Emission spectra in toluene in the presence of different amount of DBU upon an excitation at c) 350 nm and d) 430 nm at 25 °C.

The spectroscopic data of compound **1** were recorded in aqueous solutions of pH 1.1–10.9 (Figure 2). A decrease in pH value resulted in a decrease in intensity of the absorption band at ≈420 nm and a concomitant increase in intensity of the absorption band at ≈350 nm, with an isosbestic point at 378 nm. Next, the fluorescence spectra were determined at an excitation wavelength of 430 nm for different pH values. As expected from the absorption spectra, the emission intensity decreased as the pH of the solution was lowered. From this study, it appears that the phenolate ion (i.e., the most fluorescent species) is the predominant form at pH values higher than 6.0, which corresponds to the pK_a value that was calculated from the absorbance values at 420 nm at different pH values (see the Supporting Information). To quantify this trend more precisely, the fluorescence quantum yield of compound **1** was measured at different pH values (pH 2.2–10.9, Table 1). Under an excitation wavelength of 430 nm, acceptable quantum yields were observed for pH values higher than 5.6. Following these encouraging results, the photophysical properties of a series of diversely functionalized azaphthalimides were subsequently determined to assess the impact of substituents on the photoluminescence characteristics of the azaphthalimide and thus understand specific requirements for optimal fluorescence emission (entries 10–13). 2-Benzyl-subsituted pyridine systems exhibited quantum yields at pH 7.4 that were comparable to that of compound **1** (0.07–0.10, entries 11–13) with the exception of unsubstituted compound **2**, which dis-

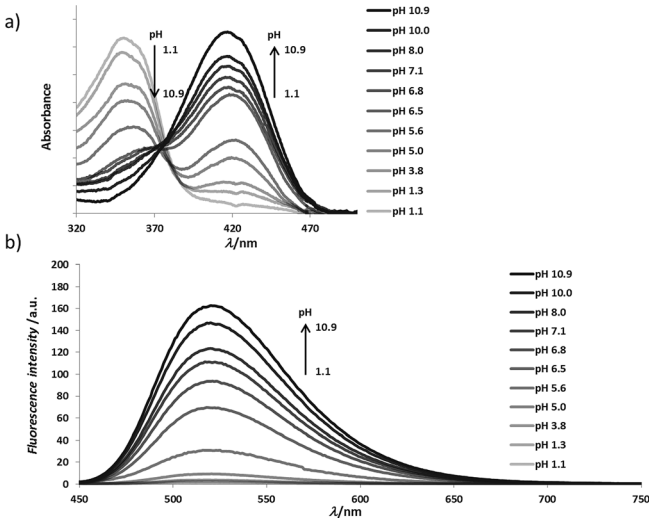

Figure 2. a) Absorption and b) emission spectra of compound **1** at 25 °C upon an excitation at 430 nm at different pH values.

Table 1. Spectroscopic behaviour of azaphthalimides **1**–**8**.

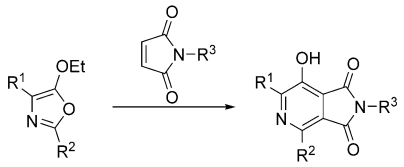

Entry	Cmpd	R^1	R^2	R^3	pH	λ_{abs} [nm][a]	λ_{em} [nm][a]	ε [$M^{-1}cm^{-1}$]	Φ_F[b]
1	**1**	Bn	Me	Me	2.2	420	522	3300	< 0.01
2					4.5	420	522	6300	0.01
3					5.6	420	522	9400	0.04
4					6.7	417	522	12900	0.08
5					7.0	418	520	14000	0.09
6					7.4	417	520	13700	0.09
7					8.5	417	520	11600	0.11
8					9.9	418	520	12000	0.09
9					10.9	417	521	10700	0.09
10	**2**	Bn	H	Me	7.4	407	513	[c]	0.02
11	**3**	Bn	CH_2Bn	Me	7.4	418	521	[c]	0.10
12	**4**	Bn	Me	Ph	7.4	421	521	[c]	0.07
13	**5**	Bn	Me	$(CH_2)_5CO_2H$	7.4	418	519	[c]	0.10
14	**6**	$(CH_2)_5CO_2H$	Me	Me	2.2	415	520	1300	0.08
15					4.5	417	518	5000	0.05
16					5.6	417	519	4700	0.07
17					6.7	415	517	5900	0.14
18					7.0	413	521	6000	0.15
19					7.4	416	517	6500	0.15
20					8.5	415	520	6000	0.17
21					9.9	415	518	6400	0.16
22					10.9	415	517	7500	0.16
23	**7**	$(CH_2)_5CONHCHPh(Et)$	Me	Me	7.4	416	518	[c]	0.16
24	**8**	$(CH_2)_5CONHCHPh(Et)$	Me	$(CH_2)_5CONHBn$	7.4	418	519	[c]	0.18

[a] λ_{abs} is the maximum of the absorption band responsible for the emission observed at λ_{em}. [b] Measurement determined at 25 °C by a relative method that used Lucifer yellow as standard ($\Phi_F = 0.21$ in water) with excitation at 430 nm. [c] Not determined.

played a markedly lower quantum yield (0.02, entry 10). Accordingly, the presence of an aliphatic group at position 6 of the pyridine ring system is crucial for fluorescence enhancement. Satisfyingly, conjugatable or conjugated hexanoic-acid-based derivatives **6**–**8** exhibited appreciable quantum yields in the range of 0.15–0.18, which is even higher than those of their 2-benzyl-substituted congeners, but with lower levels of brightness.

Applications of the fluorogenic Kondrat'eva ligation

The scope and limitations of such a fluorogenic labelling strategy were examined through four distinct applications, which are detailed hereafter.

Peptide labelling (Application 1)

The chemical modification of proteins or peptides that are only available in small quantities is generally conducted with an excess of more readily accessible labelling agents to compensate for the dilution conditions. In this context, a fluorogenic ligation reaction would advantageously avoid unwanted fluorescence emission from the unreacted starting material, which was used in excess and may not be easily removed from the product. To illustrate this point, the heptapeptide **9**, prepared through standard solid-phase synthesis, was functionalized with the maleimide **10**. The corresponding maleimide-modified heptapeptide **11** was treated with a three molar excess of oxazole **12** in NMP in the presence of 1 equivalent of TFA (Scheme 2). It is worth noting that, when in aqueous media, the Kondrat'eva ligation could proceed even in the presence of a large excess of TFA owing to the buffering effect of water; however, in organic media, TFA should not exceed one or two equivalents relative to the oxazole (see the Supporting Information). The resulting RP-HPLC analysis with UV detection of the reaction mixture clearly showed the presence of two close peaks at 9.58 and 9.63 min, which correspond to the excess of starting oxazole **12** and the azaphthalimide product **13**, respectively, and were inseparable by semi-preparative RP-HPLC (Figure 3). Advantageously, in the fluorescence detection mode, only the peak that corresponded to the azaphthalimide conjugate **13** was observed on the chromatogram (along with the peptide product in a different protonation state at 10.29 min), the unreacted oxazole peak being no longer visible.

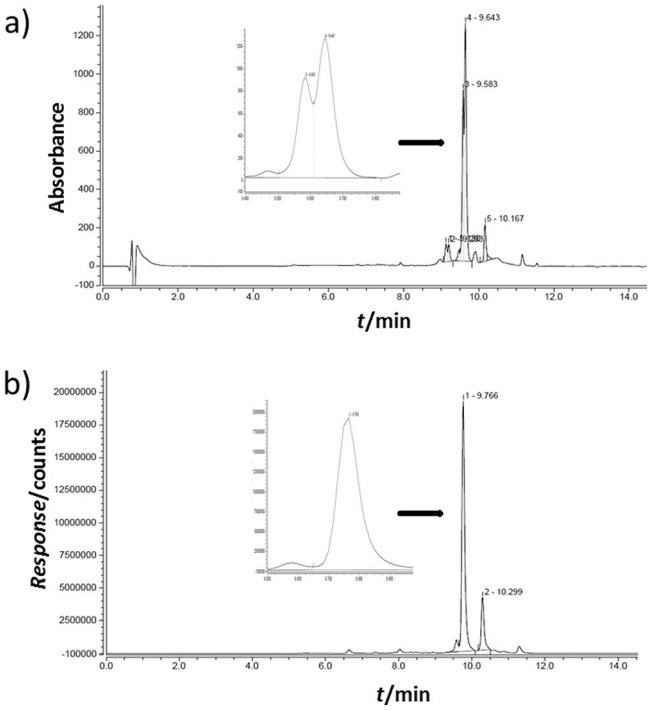

Figure 3. HPLC chromatogram of the ligation step that involves the starting materials **11** and **12** and the product **13**, in the a) UV and b) fluorescence (λ_{ex} = 420 nm, λ_{em} = 520 nm) detection mode.

Synthesis of a coumarin–azaphthalimide-based FRET cassette (Application 2)

Fluorescent or fluorogenic molecular systems have become very popular chemical tools in diverse fields of research, such as in medicinal chemistry for the determination of enzymatic activity or in chemical biology for real-time monitoring and

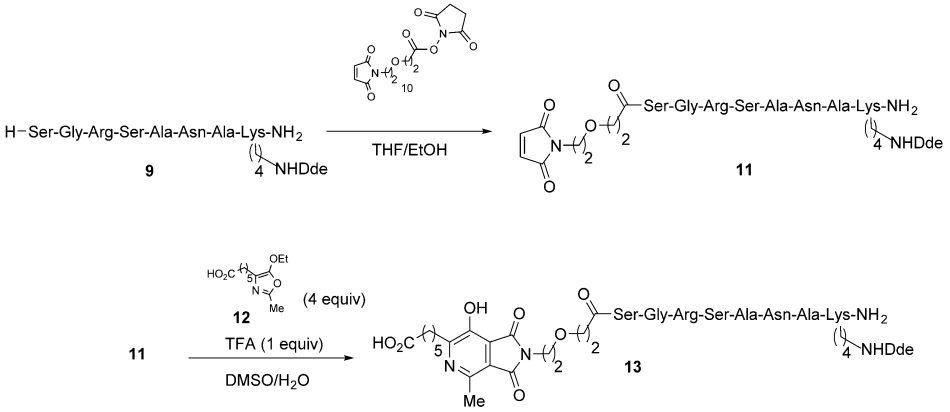

Scheme 2. Synthetic route to fluorescent peptide **13** from peptide **11** and oxazole **12**.

imaging of biological events. In this respect, the spectrum of use of azaphthalimide dyes for fluorescence applications was explored through the design of three different FRET-based probes. Such molecular systems involve a donor fluorophore, which transfers its excitation energy to a nearby acceptor chromophore (fluorophore or quencher) in a nonradiative manner. To optimize the FRET process, the donor emission spectrum should significantly overlap the acceptor absorption spectrum. Initially, the construction of a FRET cassette was investigated through the covalent attachment of two fluorophores that displayed substantial spectral overlap (see the Supporting Information): a coumarin dye **14** as the donor, recently reported by us,[19] and an azaphthalimide scaffold **6** as the acceptor (Scheme 3). Complete photophysical properties of the corresponding FRET pair **16**, which was obtained in 90% yield from compound **15**, were determined to establish whether the spectral properties of each fluorophore were preserved upon their conjugation. The UV/Vis absorption spectrum of the FRET cassette **16** showed two absorption maxima at 325 and 420 nm, which is in accordance with the sum of absorption bands of the parent dyes (Figure 4).

As expected from the FRET strategy, the azaphthalimide dye could now be selectively excited at 315 nm, while allowing emission in the green region of the spectrum (Figure 4c, dotted curve). Thus, a large pseudo-Stokes shift of 195 nm was observed, which advantageously avoids any self-absorption phenomenon that standard fluorophores may suffer from. Moreover, the energy-transfer efficiency (ETE) was found to be 77%, which demonstrates the successful combination of these two fluorophores, although significant residual fluorescence attributed to the coumarin moiety was still observed at 325 nm. This latter result highlights the difference in fluorescence efficiency between those two fluorophores.

Synthesis of an azaphthalimide–tetrazine-based smart probe (Application 3)

The preparation of a bioorthogonal smart probe based on a novel fluorophore/quencher FRET pair was envisioned. In this approach, the enhancement in fluorescence emission intensity was selectively triggered through a bioorthogonal process. Accordingly, this recent labelling strategy enabled direct fluorescence imaging of diverse biological targets without the removal of excess unreacted probe by several washing steps. Although significant progress has been made in the development of tetrazine-based smart probes by using BODIPY, coumarin, or fluorescein fluorophores, we seized the opportunity to increase their limited number, specifically by using a readily accessible fluorogenic probe.

Tetrazine **17** displays an absorption maximum of ≈521 nm, which also corresponds to the emission maximum of the azaphthalimide ring system. Consequently, a tetrazine–azaphthalimide-based FRET probe was envisioned and achieved through a final amide bond formation step between the amino tetrazine **17** and the carboxylic acid moiety of the azaphthalimide **18** (Scheme 4). With the probe in hand, its fluorogenic behaviour was explored through the inverse-electron-demand Diels–Alder cycloaddition with the strained alkene norbornene **20** in phosphate-buffered saline (PBS, pH 7.4) at room temperature. Satisfyingly, a significant fourfold fluorescence turn-on response was observed at 520 nm within 10 min of the reaction commencement (Figure 5). This result demonstrates that the fluorescence of the azaphthalimide scaffold could be quenched by the tetrazine core, presumably through a FRET mechanism. Thus, reaction of the tetrazine moiety with the strained alkene could be directly followed in real time through the fluorescence recovery of the

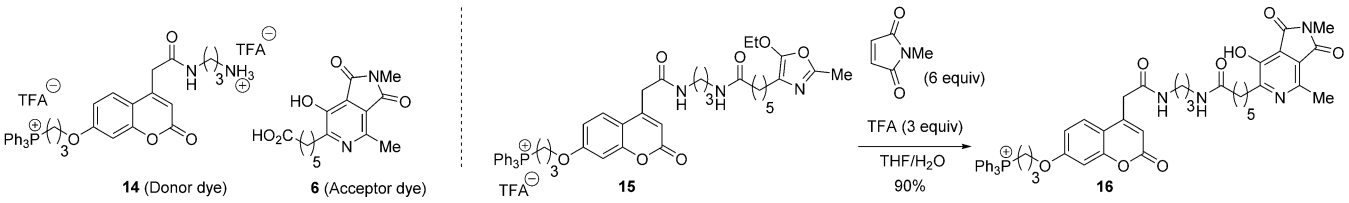

Scheme 3. Preparation of the coumarin–azaphthalimide-based FRET cassette **16**.

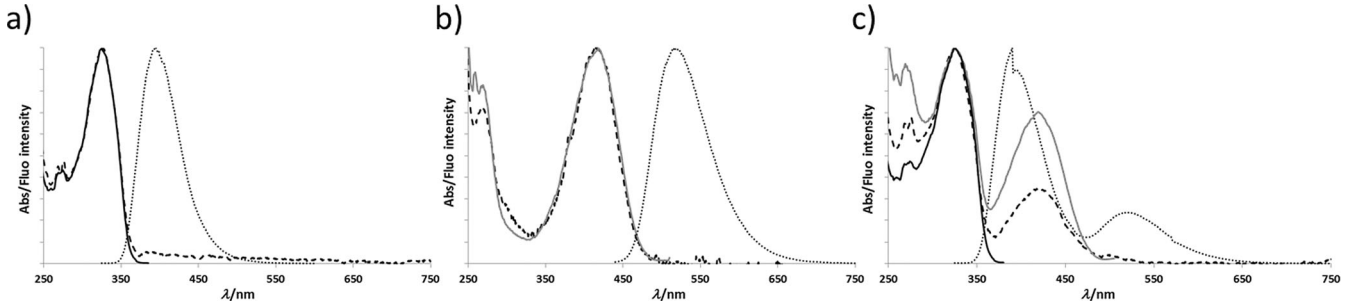

Figure 4. Normalized absorption (dashed line), emission (dotted line, $\lambda_{ex}=315$ nm for compounds **14** (a), **16** (c) and $\lambda_{ex}=430$ nm for compound **6** (b)), and excitation spectra (black line, $\lambda_{em}=395$ nm for compounds **14** (a), **16** (c); grey line, $\lambda_{em}=520$ nm for compounds **6** (b), and **16** (c)) in PBS pH 7.4 at 25 °C.

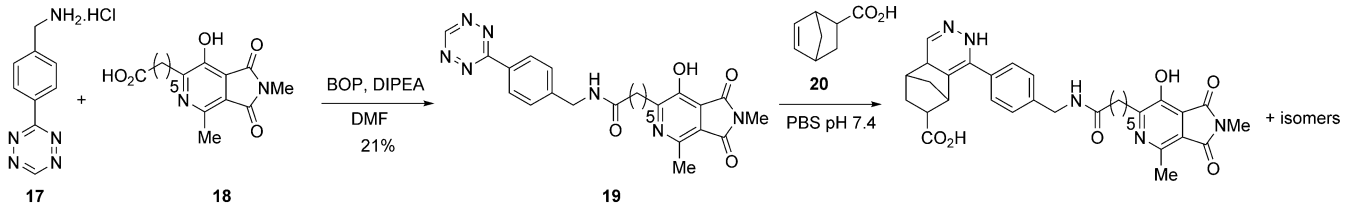

Scheme 4. Preparation of the azaphthalimide–tetrazine conjugate **19**.

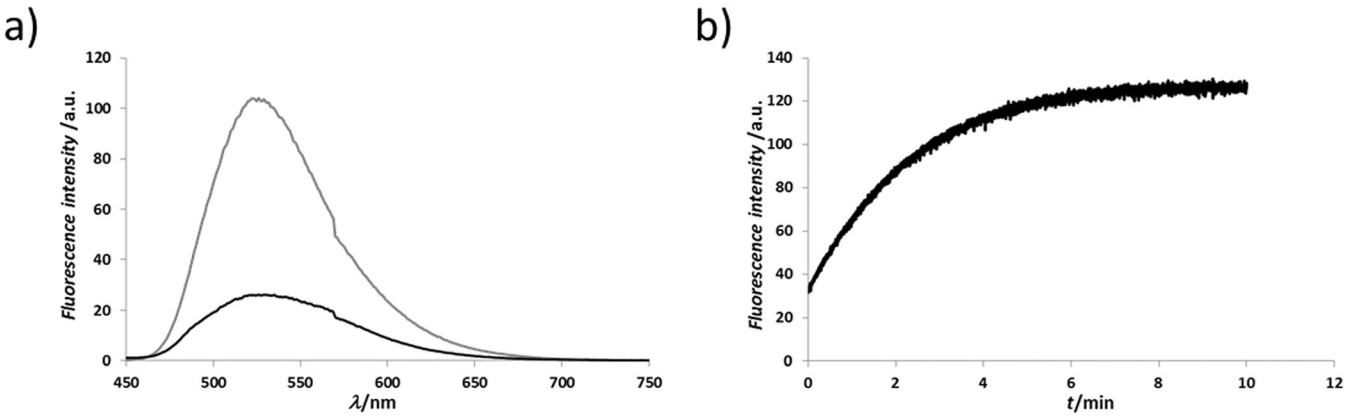

Figure 5. a) Fluorescence emission spectrum ("Scan" mode, $\lambda_{ex}=420$ nm) of probe **19** before (black) and after (grey) addition of a 3-fold excess of norbornene. b) Fluorogenic activation time course ("kinetic" mode, $\lambda_{ex}=420$ nm, $\lambda_{em}=520$ nm) of probe **19** in PBS pH 7.4 at 25 °C.

azaphtalimide moiety. Notably, probe **19** could advantageously be used to compare the kinetics of tetrazine-based Diels–Alder reactions with various dienophiles.[20]

Synthesis of a fluorogenic substrate of urokinase (Application 4)

The final investigation relied upon the preparation of a FRET-based urokinase-plasminogen-activator(uPA)-sensitive probe; uPA is a diagnostically relevant serine protease owing to its overexpression in breast and prostate cancer. Accordingly, the fluorogenic probe **24**, which constituted a FRET pair of an azaphthalimide fluorophore and a newly prepared dabcyl-like quencher **21**[21] that were connected at both ends of octapeptide H–Ser–Gly–Arg–Ser–Ala–Asn–Ala–Lys–NH_2 (known uPA substrate),[16,22] was prepared in three steps from compound **9**. During the first two steps, the diazo quencher **21** and the maleimide **10** were consecutively attached at the N- and C-terminal of the octapeptide, respectively. Then, the hetero-Diels–Alder reaction of intermediate **23** with the oxazole **12** afforded the corresponding conjugate in 38% yield. The structure of the resulting probe was unambiguously confirmed by HRMS analysis (Scheme 5).

Results obtained from the proteolysis of the fluorogenic probe **24** with commercial uPA are summarized in Figure 6. Even though an important quenching of fluorescence was observed before the enzymatic digestion, the fluorescence was completely recovered in the presence of uPA within 30 min. The quenching efficiency (QE) was determined to be 93%, which issued a satisfying ten-fold increase in fluorescence at 520 nm after enzymatic digestion (Figure 6).

Conclusion

This study reports the detailed photophysical properties of the azaphthalimide, a green-emitting moiety that was generated through the ligation of the nonfluorescent oxazole and maleimide moieties. This work demonstrated that azaphthalimides display solvatochromic character owing to hydrogen-bonding interactions with the solvent, for which the most fluorescent species (i.e., phenolate) is favored in polar or basic media as well as in physiological conditions. Finally, the albeit moderate fluorescence behaviour of azaphthalimides has found useful applications, in particular for the construction of fluorogenic FRET-based probes to target specific enzymatic activities or to evaluate the efficacy of bioconjugate processes, such as the tetrazine ligation. The latter application is currently being investigated in our group.

Experimental Section

General information

Flash column chromatography purifications were performed on silica gel (40–63 mm). Thin-layer chromatography (TLC) were carried out on Merck DC Kieselgel 60 F-254 aluminum sheets. The spots were visualized by illumination with a UV lamp (at 254/365 nm) and/or staining with $KMnO_4$ solution. Unless otherwise

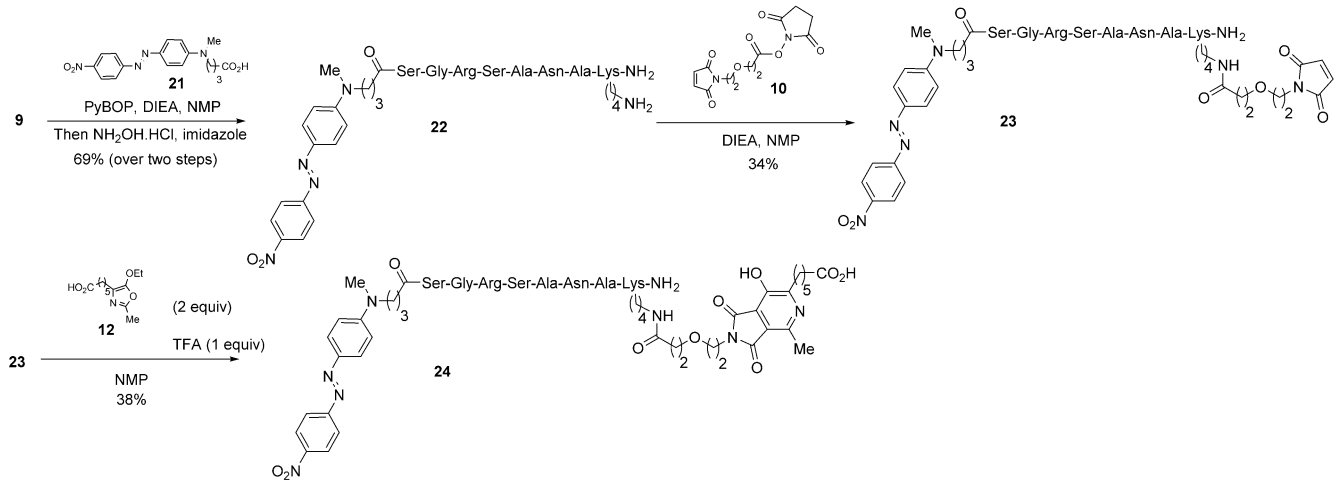

Scheme 5. Synthesis of probe **24.**

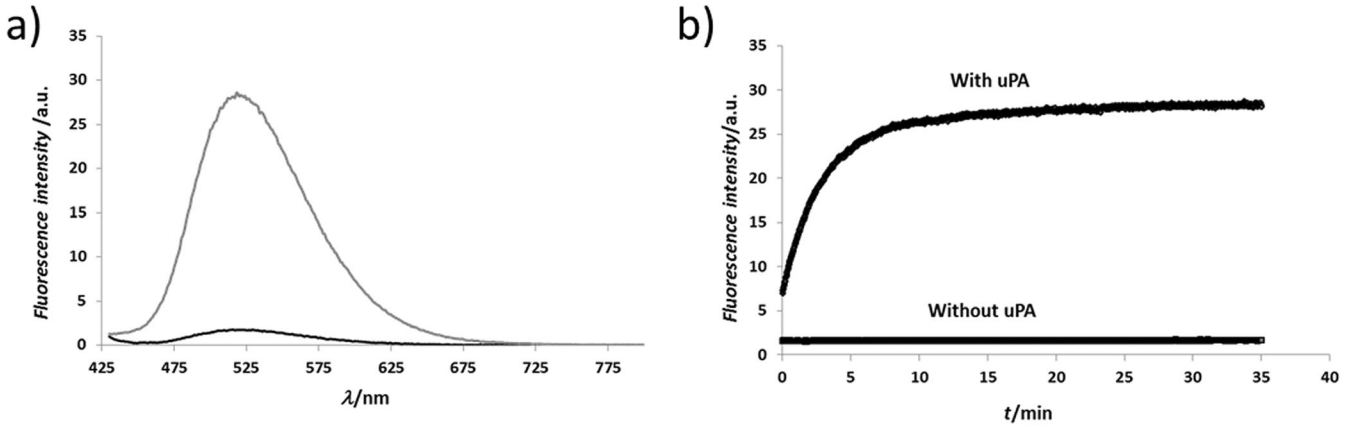

Figure 6. a) Fluorescence emission spectrum ("Scan" mode, $\lambda_{ex}=420$ nm) of probe **24** before (black) and after (grey) incubation with uPA in PBS pH 7.4 at 37 °C. b) Fluorogenic activation time course ("kinetic" mode, $\lambda_{ex}=420$ nm, $\lambda_{em}=520$ nm) of probe **24** in PBS pH 7.4 at 37 °C.

noted, all chemicals were used as received from commercial sources without further purification. PBS (pH 7.4, 0.1 M), carbonate buffer (pH 10.89, 0.1 M), and aq. mobile phases for HPLC were prepared with water that was purified by means of a MilliQ system (purified to 18.2 MΩ cm).

Instrument and methods

^{1}H and ^{13}C NMR spectra were recorded on a 300 MHz spectrometer. Chemical shifts are expressed in parts per million [ppm] by using the residual solvent peak for calibration. *J* values are expressed in Hz. High resolution mass spectra (HRMS) were obtained by using an orthogonal acceleration time-of-flight (oa-TOF) mass spectrometer equipped with an electrospray source in positive and negative modes. Low resolution mass spectra (LRMS) were obtained with a mass spectrometer equipped with an ESI source. UV/Vis absorption spectra were obtained by using a rectangular quartz cell (standard cell, Open Top, 10×10 mm, chamber volume = 3.5 mL). Fluorescence spectroscopic studies (emission/excitation spectra) were performed by using a semi-micro quartz fluorescence cell (Hellma, 104F-QS, 10×4 mm, chamber volume = 1.4 mL for quantum yields determination, chamber volume = 3.5 mL for all other studies). In vitro fluorescence assays and in vitro enzymatic assays were performed by using an ultra-micro quartz cell (Hellma, 105.251-QS, 20×3 mm, chamber volume = 45 μL). Excitation/emission spectra were recorded under the same conditions after emission/excitation at the corresponding wavelength (520/430 nm, excitation and emission filters: auto, excitation and emission slit = 5 nm). Fluorescence quantum yields were measured at 25 °C by a relative method that used Lucifer yellow ($\Phi_F=21\%$ in water, 430 nm) as a standard.[23] The following Equation (1) was used to determine the relative fluorescence quantum yield in which *A* is the absorbance (in the range of 0.01–0.1 a.u.), *F* is the area under the emission curve, *n* is the refractive index of the solvents (at 25 °C) used in measurements, and the subscripts s and x represent standard and unknown, respectively.

$$\Phi_F(X) = (A_s/A_x)\,(F_x/F_s)\,(n_x/n_s)^2\,\Phi_F(S) \quad (1)$$

The following refractive index values were used: 1.337 for PBS, 1.333 for water, 1.362 for EtOH, 1.497 for toluene, 1.424 for CH_2Cl_2, 1.344 for MeCN, 1.407 for THF, 1.328 for MeOH, 1.431 for DMF, and 1.478 for DMSO.

Preparation of the carbonate buffer (pH 10.89, 0.1 M)

500 mL of a 0.1 M solution of $NaHCO_3$ and 500 mL of a 0.1 M solution of $Na_2CO_3{\cdot}10H_2O$ were prepared. 0.1 M solution of $NaHCO_3$ (50 mL) was added to the 0.1 M solution of $Na_2CO_3{\cdot}10H_2O$ (450 mL) to give, after the pH value was adjusted by using a pH-meter, the carbonate buffer (pH 10.89, 0.1 M).

HPLC systems used for purity control or purification

Analytical HPLC

System QC1: Accucore C18 column (2.1×150 mm) with MeCN ammonium acetate buffer (20 mM, pH 7.0) as a linear gradient over 35 min from 10–90% of MeCN at a flow rate of 0.4 mL min^{-1} and injection volume of 1 μL. UV/Vis wavelength used for the absorbance detection was performed at 230 nm, and UV/Vis wavelength used for the fluorescent detection was performed at 420 nm for excitation and 520 nm for emission.

System QC: Thermo Hypersyl GOLD C18 column (5 μm, 2.1× 100 mm) with MeCN and 0.1% aq. TFA as eluents (0% MeCN for 5 min followed by 0–100% MeCN for 40 min) at a flow rate of 0.25 mL min^{-1}.

Semi-preparative HPLC

Several chromatographic systems were used for the purification steps:

System A: RP-HPLC (Varian Kromasil C18 column, 10 μm, 10.0× 250 mm) with MeCN and 0.1% aq. TFA as eluents (0% MeCN for 5 min, 0–30% MeCN for 30 min, an isocratic mixture of 30% MeCN for 15 min, and 30–100% of MeCN for 55 min) at a flow rate of 7 mL min^{-1}. UV/Vis wavelength used for the detection was performed at 465 nm.

System B: RP-HPLC (Varian Kromasil C18 column, 10 μm, 21.2× 250 mm) with MeCN and 0.1% aq. TFA as eluents (0% MeCN for 5 min, 0–100% MeCN for 100 min, and 100% MeCN for 45 min) at a flow rate of 20 mL min^{-1}. UV/Vis wavelength used for the detection was performed at 570 and 430 nm.

System C: RP-HPLC (Thermo Hypersil GOLD C18 column, 5 μm, 10.0×250 mm) with MeCN and 0.1% aq. TFA as eluents (0% MeCN for 10 min, 0–100% MeCN for 200 min, and 100% MeCN for 30 min) at a flow rate of 4 mL min^{-1}. UV/Vis wavelength used for the detection was performed at 575 and 390 nm.

System D: RP-HPLC (Varian Kromasil C18 column, 10 μm, 21.2× 250 mm) with MeCN and 0.1% aq. TFA as eluents (0% MeCN for 10 min, 0–100% MeCN for 100 min, and 100% MeCN for 20 min) at a flow rate of 20 mL min^{-1}. UV/Vis wavelength used for the detection was performed at 330 and 235 nm.

System E: RP-HPLC (Varian Kromasil C18 column, 10 μm, 21.2× 250 mm) with MeCN and 0.1% aq. TFA as eluents (0% MeCN for 10 min, 0–100% MeCN for 100 min, and 100% MeCN for 20 min) at a flow rate of 20 mL min^{-1}. UV/Vis wavelength used for the detection was performed at 365 and 310 nm.

System F: RP-HPLC (Varian Kromasil C18 column, 10 μm, 21.2× 250 mm) with MeCN and 0.1% aq. TFA as eluents (0% MeCN for 10 min, 0–100% MeCN for 200 min, and 100% MeCN for 30 min) at a flow rate of 20 mL min^{-1}. UV/Vis wavelength used for the detection was performed at 355 and 235 nm.

System G: RP-HPLC (Varian Kromasil C18 column, 10 μm, 21.2× 250 mm) with MeCN and 0.1% aq. TFA as eluents (0% MeCN for 5 min, 0–20% MeCN for 20 min, 20–60% MeCN for 80 min, and 60–100% MeCN for 35 min) at a flow rate of 20 mL min^{-1}. UV/Vis wavelength used for the detection was performed at 340 and 240 nm.

Synthesis of azaphthalimide peptide conjugate 13

Step 1: a) *N*-Hydroxysuccinimide (211 mg, 1.83 mmol, 1.1 equiv) and EDCI·HCl (351 mg, 1.83 mmol, 1.1 equiv) were added to a solution of maleimide carboxylic acid **10**[24] (355 mg, 1.67 mmol, 1 equiv) in a mixture of dry THF/EtOH (6 mL, 1:1 v/v). The resulting reaction mixture was stirred at room temperature until reaction completion (cycloexane/EtOAc 50:50). The solution was quenched with a saturated solution of $NaHCO_3$, extract with CH_2Cl_2 (2× 20 mL). The combined organic phases were washed with brine, dried over $MgSO_4$, concentrated under vacuum, and used in the next step without further purification. b) The TFA salt of the heptapeptide **9**[16] (20 mg, 18.7 μmol, 1 equiv) and *N*-hydroxysuccinimide-activated maleimide **10** (7 mg, 22.5 μmol, 1.2 equiv) were dissolved in NMP (330 μL). DIEA (2.0 M solution in NMP, 26.1 μL, 0.15 mmol, 8 equiv) was added, and the resulting reaction mixture was stirred at RT for 2 h. The reaction progress was monitored by RP-HPLC (System QC). After the reaction was completed, Et_2O was added, and the resulting precipitate was centrifuged. The precipitate that contained the maleimide-modified peptide was collected and used without further purification in the next step, because we found that the conjugate was not stable during purification on semi-preparative RP-HPLC

Step 2: 5-Ethoxyoxazole **12**[16] (18 mg, 74.8 μmol, 4 equiv) and a solution of TFA (1.43 μL, 18.7 μmol, 1 equiv) in water (210 μL) was added to the peptide–maleimide conjugate, which was obtained in Step 1, dissolved in DMSO (420 μL), and the reaction mixture was stirred at RT for 5 h. The reaction progress was monitored by RP-HPLC (System QC). The mixture was diluted with aq. 0.1% TFA and purified by semi-preparative RP-HPLC, and the product-containing fractions were lyophilized (System F). To remove the excess oxazole, which was not separable from the azaphthalimide product by semi-preparative RP-HPLC, Et_2O was added to the lyophilisate, the resulting precipitate was centrifuged, and the product-containing fractions were lyophilized to give 10.5 mg (42% yield for the two steps) of the azaphthalimide-labelled peptide **13** as a yellow amorphous powder. UV/Vis (PBS): $\lambda_{max}=417$ nm; HPLC (System QC): $t_R=21.883$ min (93% purity).

Synthesis of the coumarin FRET pair 16

Compounds **14** and **15** were prepared according to a reported procedure.[24]

Compound 16

TFA (2.78 μL, 35.9, 3 equiv) and *N*-methylmaleimide (8 mg, 72.0 μmol, 6 equiv) were added successively to a solution of azaphthalimide **15** (11 mg, 12.0 μmol) in a H_2O/THF mixture (72 μL, 1:1). The solution was stirred at RT for 18 h and directly purified by semi-preparative RP-HPLC (System G). The product-containing fractions were lyophilized to afford the product (12 mg, 90% yield) as a yellow oil. ^{1}H NMR (300 MHz, [D$_4$]MeOD): $\delta=7.95$–7.71 (m, 15H), 7.69 (dd, $J=8.7$, 3.9 Hz, 1H), 7.01–6.93 (m, 1H), 6.93–6.86 (m, 1H), 6.27 (s, 1H), 4.25 (d, $J=4.9$ Hz, 2H), 3.75 (s, 2H), 3.68–3.56 (m, 2H), 3.25–3.14 (m, 4H), 3.06 (s, 3H), 2.92–3.82 (m, 2H), 2.67 (s, 3H), 2.24–2.13 (m, 4H), 1.77–1.55 (m, 6H), 1.41–1.26 ppm (m, 4H); ^{13}C NMR (75 MHz, [D$_4$]MeOD): $\delta=176.2$, 170.8, 168.7, 163.0, 163.0, 162.9, 156.6, 156.6, 152.2, 146.9, 146.5, 136.4 (d, $J_{P-C}=2.9$ Hz, 3C), 134.9 (d, $J_{P-C}=10.1$ Hz, 6C), 131.6 (d, $J_{P-C}=12.7$ Hz, 6C), 127.6, 122.5, 122.3, 119.7 (d, $J_{P-C}=86.9$ Hz, 3C), 114.5, 114.5, 113.9, 102.7,

68.5 (d, J_{P-C} = 16.5 Hz, 1C), 40.1, 38.1, 37.6, 36.9, 33.2, 30.1, 30.0, 29.0, 26.7, 23.9, 23.5 (d, J_{P-C} = 3.0 Hz, 1C), 20.0 (d, J_{P-C} = 53.7 Hz, 1C), 19.5 ppm; IR (neat): $\tilde{\nu}$ = 3363, 2942, 2509, 1672, 1611, 1543, 1438, 1385, 1280, 1201, 1178, 1134, 1114 cm^{-1}; HRMS (ESI^+): *m/z* calcd for $C_{50}H_{52}N_4O_8P$: 867.3523 $[M]^+$; found: 867.3499; HPLC (System QC): t_R = 27.3 min, purity 97.5%.

Synthesis of the fluorogenic tetrazine-based probe 19

Compound 19

BOP ((Benzotriazol-1-yloxy)tris(dimethylamino)phosphonium hexafluorophosphate) (29.2 mg, 0.066 mmol, 1.01 equiv), benzylamine tetrazine **17**[25] (16.1 mg, 0.0718 mmol, 1.1 equiv), and DIEA (46 μL, 0.26 mmol, 4 equiv) were added to a solution of azaphthalimide **6** (20.0 mg, 0.0653 mmol, 1 equiv) in dry DMF (400 μL), and the reaction was stirred at RT for 2 h. Upon reaction completion, the crude product was purified by flash-column chromatography (silica gel, EtOAc 100% to Acetone 100%). The residue was diluted with aq 0.1% TFA and purified by semi-preparative RP-HPLC (System E). The product-containing fractions were lyophilized to give the product (6.6 mg, 21%) as an orange amorphous powder. M.p. 122 °C; ^1H NMR (300 MHz, $CDCl_3$): δ = 10.58 (s, 1H), 8.55–8.28 (m, 3H), 7.52 (d, J = 8.4 Hz, 2H), 4.39 (d, J = 5.9 Hz, 3H), 2.97 (s, 3H), 2.87–2.78 (m, 2H), 2.61 (s, 2H), 2.19 (t, J = 7.3 Hz, 2H), 1.71–1.51 (m, 4H), 1.42–1.28 ppm (m, 2H); ^{13}C NMR (75 MHz, $CDCl_3$): δ = 172.3, 168.1, 166.6, 165.4, 159.90, 158.1, 145.1, 130.3, 128.1, 128.1, 127.8, 127.8, 121.0, 79.4, 78.9, 78.5, 41.82, 35.3, 32.2, 28.6, 27.3, 25.1, 23.60, 19.6 ppm; IR (neat): $\tilde{\nu}$ = 3279, 2925, 2852, 1697, 1661, 1607, 1515, 1436, 1348, 1251, 1178 cm^{-1}; HRMS (ESI) *m/z* calcd for $C_{24}H_{25}N_7O_4$: 475.1968 $[M+H]^+$; found: 476.2045; HPLC (System QC): t_R = 23.15 min (96.3% purity).

Preparation of the uPA-responsive probe 24

4-(methyl(4-((4-nitrophenyl)diazenyl)phenyl)amino)butanoic acid 21

$NOBF_4$ (187.7 mg, 1.59 mmol, 1.1 equiv) was added to a solution of *para*-nitroaniline (200 mg, 1.45 mmol, 1 equiv) in freshly distilled CH_3CN (2 mL) cooled to 0 °C. The resulting reaction mixture was stirred at 0 °C for 15 min. A solution of 4-(methyl-phenyl-amino)-butyric acid (308 mg, 1.59 mmol, 1.1 equiv) in freshly distilled CH_3CN (1 mL) was added dropwise, and the resulting mixture was stirred for 30 min at RT. Aq. 0.1 M acetate buffer (pH 5.0) was added slowly until a precipitate appeared. The red solid was recovered by filtration and washed with a mixture of H_2O/CH_3CN (1:1) and Et_2O. The crude product was purified by flash column chromatography (silica gel, cyclohexane/EtOAc 60:40–40:60–0:100 then EtOAc/MeOH 90:10). The product (108 mg, 22%) was isolated as a red powder. M.p. 194 °C; ^1H NMR (300 MHz, [D_6]DMSO): δ = 8.36 (d, J = 9.1 Hz, 2H), 7.93 (d, J = 9.1 Hz, 2H), 7.85 (d, J = 9.1 Hz, 2H), 6.90 (d, J = 9.1 Hz, 2H), 3.55–3.44 (t, J = 7.2 Hz, 2H), 3.08 (s, 3H), 2.37–2.17 (t, J = 7.2 Hz, 2H), 1.91–1.67 ppm (q, J = 7.2 Hz, 2H); ^{13}C NMR (75 MHz, [D_6]DMSO): δ = 174.2, 156.3, 152.6, 146.8, 142.7, 126.0, 125.0, 122.5, 111.6, 50.9, 38.3, 30.7, 21.9 ppm; UV/Vis (DMSO, 25 °C): λ_{max} abs = 500 nm; IR (neat): $\tilde{\nu}$ = 3285, 2921, 2107, 1691, 1601, 1506, 1422, 1289, 1214, 1024, 858, 823, 755, 685, 534, 410 cm^{-1}.

uPA-responsive probe 24

Step 1: The TFA salt of the heptapeptide **9** (20 mg, 18.7 μmol, 1 equiv), the quencher **21** (8 mg, 23.4 μmol, 1.1 equiv), and PyBOP (12.0 mg, 23.4 μmol, 1.1 equiv) were dissolved in NMP (280 μL). DIEA (2.0 M solution in NMP, 18 μL, 104 μmol, 5 equiv) was added, and the resulting reaction mixture was stirred at RT for 2 h. The reaction completion was checked by RP-HPLC (System QC). Upon reaction completion, Et_2O was added, the resulting precipitate was centrifuged and dissolved in DMF (2 mL). Hydroxylamine hydrochloride (6.8 mg, 104 μmol, 5 equiv) and imidazole (7.2 mg, 104 μmol, 5 equiv) were added, and the reaction mixture was stirred overnight at RT. The reaction progress was monitored by RP-HPLC (System QC). After reaction completion, the mixture was diluted with aq 0.1% TFA and purified by semi-preparative RP-HPLC (System B). The product-containing fractions were lyophilized to give the modified peptide **22** (15.96 mg, 69% overall yield for the two steps) as a red amorphous powder. LRMS (ESI): *m/z* calcd for $C_{47}H_{72}N_{18}O_{14}$: 1113.2050 $[M+H]^+$; found: 1113.13; UV/Vis (PBS): λ_{max} = 500 nm, HPLC (System QC): t_R = 24.48 min (93.6% purity).

Step 2: Peptide **22** (2.78 mg, 2.3 μmol, 1 equiv) and *N*-hydroxysuccinimide activated maleimide **10** (0.85 mg, 2.7 μmol, 1.2 equiv) were dissolved in NMP (40 μL). DIEA (2.0 M solution in NMP, 3.2 μL, 18.2 μmol, 8 equiv) was added, and the resulting reaction mixture was stirred at RT for 2 h 30 min. The reaction progress was monitored by RP-HPLC (System QC). Upon reaction completion, the mixture was diluted with aq 0.1% TFA and purified by semi-preparative RP-HPLC (System A). The product-containing fractions were lyophilized to give the maleimide-functionalized peptide **23** (1.0 mg, 34%) as a red amorphous powder. LRMS (ESI^+) *m/z* calcd for $C_{56}H_{81}N_{19}O_{18}$: 1308.38 $[M+H]^+$; found: 1308.47; UV/Vis (PBS): $\lambda_{abs(max)}$ = 500 nm; HPLC (System QC): t_R = 25.63 min (87.8% purity).

Step 3: 5-Alkoxyoxazole **12** (0.80 mg, 3.1 μmol, 2 equiv),[16] maleimide-modified peptide **23** (2.2 mg, 1.55 μmol, 1 equiv) in NMP (39 μL), and TFA (0.124 μL, 155 μmol, 1 equiv) were combined and stirred at RT for 3 h. The reaction progress was monitored by RP-HPLC (System QC). Upon reaction completion, the mixture was diluted with aq 0.1% TFA and purified by semi-preparative RP-HPLC (System C). The product-containing fractions were lyophilized to give the fluorogenic probe **24** (1.05 mg, 38%) as a red amorphous powder. HRMS (ESI^+) *m/z* calcd for $C_{66}H_{95}N_{20}O_{21}$: 1503.6981 $[M+H]^+$; found: 1503.7013; UV/Vis (PBS): λ_{max} = 500 nm. HPLC (System QC): t_R = 26.026 min (> 99% purity).

Fluorogenic bioorthognal reaction between norbonene and tetrazine–azaphthalimide conjugate 19

A solution of norbornene (5 μL, 360 mM in DMSO) was added to a 10 mM solution of fluorogenic probe **19** in PBS (45 μL, 0.1 M pH 7.4) in the ultra-micro quartz cell. After excitation at the desired wavelength (420 nm), the fluorescence emission at 520 nm was simultaneously monitored over time, with measurements recorded every 0.1 s. Emission spectra of the probe were recorded before and after the reaction to determine the quenching efficiency (QE), which was calculated on the basis of the following equation: QE = 100 × [1 − (fluorescence emission intensity of the probe)/(fluorescence emission intensity of the probe after compete reaction of tetrazine moiety)]

In vitro enzymatic assays - fluorescence bioassays

A 100 μM solution of fluorogenic peptide **24** was prepared in PBS (45 μL, 0.1 M pH 7.4) and transferred into the ultra-micro quartz cell. uPA solution (10 μL, 1.2 U, 25 μg in 100 μL of buffer: 500 mM Tris·HCl + 1.0 M NaCl + 1% PEG 6000 + 2.0 M mannitol) was added, and the resulting mixture was incubated at 37.5 °C for 30 min. After excitation at the desired wavelength (420 nm), the fluorescence emission at 520 nm was monitored over time, with measure-

ments recorded every 1 s. Emission spectra of the probe were recorded before and after cleavage to determine the quenching efficiency (QE), which was calculated on the basis of the following equation: QE = 100 × [1 − (fluorescence emission intensity of the probe)/(fluorescence emission intensity of the probe after compete digestion by uPA)].

Acknowledgements

We thank the Region Haute-Normandie (FEDER CHIMBIO HN 0001401) for financial support to K.R. This work was also partially supported by the Centre National de la Recherche Scientifique (CNRS), INSA Rouen, Rouen University, and the Labex SynOrg (ANR-11-LABX-0029). We also thank Emilie Petit (INSA de Rouen) and Laetitia Bailly (INSA de Rouen) for HPLC analyses and Albert Marcual (CNRS) for HRMS analyses.

Keywords: azaphthalimide · Diels–Alder · fluorescence spectroscopy · ligation · oxazole

[1] a) C. P. R. Hackenberger, D. Schwarzer, *Angew. Chem. Int. Ed.* **2008**, *47*, 10030 – 10074; *Angew. Chem.* **2008**, *120*, 10182 – 10228; b) S. Liu, K. T. Dicker, X. Jia, *Chem. Commun.* **2015**, *51*, 5218.

[2] H. C. Kolb, M. G. Finn, K. B. Sharpless, *Angew. Chem. Int. Ed.* **2001**, *40*, 2004 – 2021; *Angew. Chem.* **2001**, *113*, 2056 – 2075.

[3] a) D. Rideout, *Science* **1986**, *233*, 561 – 563; b) V. W. Cornish, K. M. Hahn, P. G. Schultz, *J. Am. Chem. Soc.* **1996**, *118*, 8150 – 8151; c) O. El-Mahdi, O. Melnyk, *Bioconjugate Chem.* **2013**, *24*, 735 – 765; d) S. Ulrich, D. Boturyn, A. Marra, O. Renaudet, P. Dumy, *Chem. Eur. J.* **2014**, *20*, 34 – 41.

[4] E. Saxon, C. R. Bertozzi, *Science* **2000**, *287*, 2007.

[5] a) C. W. Tornøe, C. Christensen, M. J. Meldal, *J. Org. Chem.* **2002**, *67*, 3057 – 3064; b) V. V. Rostovtsev, L. G. Green, V. V. Fokin, K. B. Sharpless, *Angew. Chem. Int. Ed.* **2002**, *41*, 2596 – 2599; *Angew. Chem.* **2002**, *114*, 2708 – 2711.

[6] N. J. Agard, J. A. Prescher, C. R. Bertozzi, *J. Am. Chem. Soc.* **2004**, *126*, 15046 – 15047.

[7] a) S. Wallace, J. W. Chin, *Chem. Sci.* **2014**, *5*, 1742 – 1744; b) L. Plougastel, O. Koniev, S. Specklin, E. Decuypere, C. Créminon, D.-A. Buisson, A. Wagner, S. Kolodych, F. Taran, *Chem. Commun.* **2014**, *50*, 9376 – 9378; c) H. Liu, D. Audisio, L. Plougastel, E. Decuypere, D.-A. Buisson, O. Koniev, S. Kolodych, A. Wagner, M. Elhabiri, A. Krzyczmonik, S. Forsback, O. Solin, V. Gouverneur, F. Taran, *Angew. Chem. Int. Ed.* **2016**, *55*, 12073 – 12077; *Angew. Chem* **2016**, *128*, 12252 – 12256.

[8] D. A. MacKenzie, A. R. Sherratt, M. Chigrinova, L. L. W. Cheung, J. P. Pezacki, *Curr. Opin. Chem. Biol.* **2014**, *21*, 81 – 88.

[9] N. K. Devaraj, R. Weissleder, S. A. Hilderbrand, *Bioconjugate Chem.* **2008**, *19*, 2297 – 2299.

[10] Q. Li, T. Dong, X. Liu, X. Lei, *J. Am. Chem. Soc.* **2013**, *135*, 4996 – 4999.

[11] a) G. Clavé, H. Volland, M. Flaender, D. Gasparutto, A. Romieu, P.-Y. Renard, *Org. Biomol. Chem.* **2010**, *8*, 4329 – 4345; b) D. M. Beal, L. H. Jones, *Angew. Chem. Int. Ed.* **2012**, *51*, 6320 – 6326; *Angew. Chem.* **2012**, *124*, 6426 – 6432; c) A. Chevalier, M. Dubois, V. Le Joncour, S. Dautrey, C. Lecointre, A. Romieu, P.-Y. Renard, H. Castel, C. Sabot, *Bioconjugate Chem.* **2013**, *24*, 1119 – 1133; d) M. Rashidian, S. C. Kumarapperuma, K. Gabrielse, A. Fegan, C. R. Wagner, M. D. Distefano, *J. Am. Chem. Soc.* **2013**, *135*, 16388 – 16396.

[12] For a review, see: P. Shieha, C. R. Bertozzi, *Org. Biomol. Chem.* **2014**, *12*, 9307 – 9320.

[13] P. I. Kitov, D. F. Vinals, S. Ng, K. F. Tjhung, R. Derda, *J. Am. Chem. Soc.* **2014**, *136*, 8149 – 8152.

[14] W. Song, Y. Wang, J. Qu, M. M. Madden, Q. Lin, *Angew. Chem. Int. Ed.* **2008**, *47*, 2832 – 2835; *Angew. Chem.* **2008**, *120*, 2874 – 2877.

[15] J. C. Jewett, C. R. Bertozzi, *Org. Lett.* **2011**, *13*, 5937 – 5939.

[16] a) L.-A. Jouanno, A. Chevalier, N. Sekkat, N. Perzo, H. Castel, A. Romieu, N. Lange, C. Sabot, P.-Y. Renard, *J. Org. Chem.* **2014**, *79*, 10353 – 10366; b) L.-A. Jouanno, K. Renault, C. Sabot, P.-Y. Renard, *Eur. J. Org. Chem.* **2016**, 3264 – 3281.

[17] For peptidic applications of Diels–Alder reactions, see : a) A. Dantas de Araújo, J. M. Palomo, J. Cramer, O. Seitz, K. Alexandrov, H. Waldmann, *Chem. Eur. J.* **2006**, *12*, 6095 – 6109; b) T. Pauloehrl, G. Delaittre, V. Winkler, A. Welle, M. Bruns, H. G. Börner, A. M. Greiner, M. Bastmeyer, C. Barner-Kowollik, *Angew. Chem. Int. Ed.* **2012**, *51*, 1071 – 1074; *Angew. Chem.* **2012**, *124*, 1096 – 1099; c) K. Hoogewijs, D. Buyst, J. M. Winne, J. C. Martins, A. Madder, *Chem. Commun.* **2013**, *49*, 2927 – 2929; d) O. Brun, X. Elduque, E. Pedroso, A. Grandas, *J. Org. Chem.* **2015**, *80*, 6093 – 6101.

[18] a) X. Liu, L. Gao, L. Yang, L. Zou, W. Chena, W. Song, *RSC Adv.* **2015**, *5*, 18177 – 18182; b) X. Liu, L. Yang, L. Gao, W. Chen, F. Qi, W. Song, *Tetrahedron* **2015**, *71*, 8285 – 8289.

[19] A. Lizzul-Jurse, L. Bailly, M. Hubert-Roux, C. Afonso, P.-Y. Renard, C. Sabot, *Org. Biomol. Chem.* **2016**, *14*, 7777 – 7791.

[20] Y.-J. Lee, Y. Kurra, Y. Yang, J. Torres-Kolbus, A. Deiters, W. R. Liu, *Chem. Commun.* **2014**, *50*, 13085.

[21] B. Roubinet, A. Chevalier, P.-Y. Renard, A. Romieu, *Eur. J. Org. Chem.* **2015**, 166 – 182.

[22] a) B. Law, A. Curino, T. H. Bugge, R. Weissleder, C.-H. Tung, *Chem. Biol.* **2004**, *11*, 99 – 106; b) R. Malik, S. Qian, B. Law, *Anal. Biochem.* **2011**, *412*, 26 – 33.

[23] P. A. Peixoto, A. Boulange, M. Ball, B. Naudin, T. Alle, P. Cosette, P. Karuso, X. Franck, *J. Am. Chem. Soc.* **2014**, *136*, 15248 – 15256.

[24] A. Warnecke, I. Fichtner, D. Garmann, U. Jaehde, F. Kratz, *Bioconjugate Chem.* **2004**, *15*, 1349 – 1359.

[25] J. Yang, M. R. Karver, W. Li, S. Sahu, N. K. Devaraj, *Angew. Chem. Int. Ed.* **2012**, *51*, 5222 – 5225; *Angew. Chem.* **2012**, *124*, 5312 – 5315.

Received: July 29, 2016
Published online on ■■ ■■, 0000

FULL PAPER

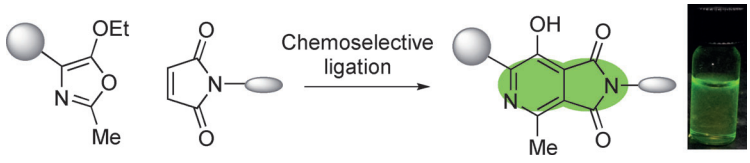

Fluorescent ligation: The fluorogenic reaction of oxazoles with maleimides and its subsequent application for the construction of FRET probes is reported.

Fluorescence Probes

*K. Renault, L.-A. Jouanno, A. Lizzul-Jurse, P.-Y. Renard, C. Sabot**

■■ – ■■

Fluorogenic Behaviour of the Hetero-Diels–Alder Ligation of 5-Alkoxyoxazoles with Maleimides and their Applications